Direct Visualization of the Enzymatic Digestion of a Single Fiber of Native Cellulose in an Aqueous Environment by Atomic Force Microscopy

ARTICLE *in* LANGMUIR · FEBRUARY 2010

Impact Factor: 4.46 · DOI: 10.1021/la9037028 · Source: PubMed

7 AUTHORS, INCLUDING:

Chris Vandenende
University of Guelph
7 PUBLICATIONS **90** CITATIONS
SEE PROFILE

Anthony J Clarke
University of Guelph
130 PUBLICATIONS **2,719** CITATIONS
SEE PROFILE

John R Dutcher
University of Guelph
175 PUBLICATIONS **3,781** CITATIONS
SEE PROFILE

Sharon G Roscoe
Acadia University
57 PUBLICATIONS **1,266** CITATIONS
SEE PROFILE

Langmuir
Article
pubs.acs.org/Langmuir

Direct Visualization of the Enzymatic Digestion of a Single Fiber of Native Cellulose in an Aqueous Environment by Atomic Force Microscopy

Amanda Quirk,[†] Jacek Lipkowski,*[,†] Chris Vandenende,[‡] Darrell Cockburn,[‡] Anthony J. Clarke,[‡] John R. Dutcher,[§] and Sharon G. Roscoe[∥]

[†]*Department of Chemistry*, [‡]*Department of Molecular and Cellular Biology*, *and* [§]*Department of Physics, University of Guelph, Guelph, Ontario, N1G 2W1 Canada, and* [∥]*Department of Chemistry, Acadia University, Wolfville, Nova Scotia, B4P 2R6 Canada*

Received September 30, 2009. Revised Manuscript Received February 3, 2010

Atomic force microscopy (AFM) was used to study native cellulose films prepared from a bacterial cellulose source, *Acetobacter xylinum*, using a novel application of the Langmuir−Blodgett technique. These films allowed high-resolution AFM images of single fibers and their microfibril structure to be obtained. Two types of experiments were performed. First, the fibers were characterized using samples that were dried after LB deposition. Next, novel protocols that allowed us to image single fibers of cellulose in films that were never dried were developed. This procedure allowed us to perform in situ AFM imaging studies of the enzymatic hydrolysis of single cellulose fibers in solution using cellulolytic enzymes. The in situ degradation of cellulose fibers was monitored over a 9 h period using AFM. These studies provided the first direct, real-time images of the enzymatic degradation of a single cellulose fiber. We have demonstrated the tremendous potential of AFM to study the mechanism of the enzymatic digestion of cellulose and to identify the most effective enzymes for the digestion of various cellulose structures or isomorphs.

Introduction

Cellulose is a linear polymer with β-(1 → 4)-linked glucose sugars varying in length up to 18 000 residues in native cellulose. The base unit of cellulose is cellobiose—two glucose sugars linked with 180° relative rotation. The arrangement of cellobiose units provides a complex system of intra- and intermolecular hydrogen bonding between residues, which contributes to the rigid structure and to fibril formation. Cellulose chains form a complex superstructure organized into micro- and macrofibrils and are the structural component of the primary cell walls of plants.

Cellulose structure has primarily been investigated using electron microscopy techniques such as transmission electron microscopy (TEM)[1,2] and scanning electron microscopy (SEM).[3] The width of the microfibril structure has been found to be 2−10 nm in diameter depending on the source of cellulose.[4] X-ray crystallography has provided structural information on the two crystalline phases of native cellulose as well as the microfibril structure.[3,5]

Electron microscopy techniques have the disadvantages of complex sample preparation and the inability to acquire in situ data. With the invention of the atomic force microscope (AFM) in 1986 by Binnig et al.,[6] new possibilities for measurements arose. AFM has the ability to acquire real-space three-dimensional data and to measure adhesive forces and mechanical properties at the molecular level. Regenerated and native cellulose films have been studied using atomic force microscopy (AFM) to obtain images of the macroscale topography of cellulose fibers[7,8] and to determine the crystal packing of cellulose chains on the nanoscale.[9−11] Image analysis has also been performed in a number of studies to determine the root-mean-square roughness[12] and thickness[12,13] of the films. AFM provides ultrahigh resolution of the cellulose samples and allows in situ degradation studies to be performed that are not possible using electron microscopy techniques.

In the preparation of model cellulose films, much attention has been paid to the nature of the interactions between cellulose and the solid substrate. Different pretreatments of mica, silica, glass, and highly oriented pyrolytic graphite (HOPG) have resulted in hydrophilic or hydrophobic surfaces that increase the adhesion of the cellulose film to the solid substrate. In the case of native cellulose films, it is important to use a hydrophilic surface[14,15] so that the cellulose fibers strongly adhere to the solid support. This is necessary to ensure that a single fiber can be monitored for the duration of the experiment without being dislodged mechanically from the substrate by the AFM tip.

The enzyme system used in the present study was CenA endoglucanase from the bacterium *Cellulomonas fimi*. CenA is a noncellulosomal family 6 endoglucanase with a molar mass of approximately 47 kDa.[16] Small-angle X-ray scattering analysis shows that CenA is "tadpole-shaped" having an elliptical head

(1) Boisset, C.; Fraschini, C.; Schulein, M.; Henrissat, B.; Chanzy, H. *Appl. Environ. Microbiol.* **2000**, *66*, 1444–1452.
(2) Bayer, E. A.; Chanzy, H.; Lamed, R.; Shoham, Y. *Curr. Opin. Struct. Biol.* **1998**, *8*, 548–557.
(3) Bohn, A.; Fink, H. P.; Ganster, J.; Pinnow, M. *Macromol. Chem. Phys.* **2000**, *201*, 1913–1921.
(4) Ohad, I.; Danon, D. *J. Cell Biol.* **1964**, *22*, 302.
(5) Wada, M.; Sugiyama, J.; Okano, T. *J. Appl. Polym. Sci.* **1993**, *49*, 1491–1496.
(6) Binnig, G.; Quate, C. F.; Gerber, C. *Phys. Rev. Lett.* **1986**, *56*, 930–933.
(7) Hanley, S. J.; Giasson, J.; Revol, J.; Gray, D. G. *Polymer* **1992**, *33*, 4639–4642.
(8) Piantanida, G.; Bicchieri, M.; Coluzza, C. *Polymer* **2005**, *46*, 12313–12321.
(9) Yan, L.; Li, W.; Yang, J.; Zhu, Q. *Macromol. Biosci.* **2004**, *4*, 112–118.
(10) Baker, A. A.; Helbert, W.; Sugiyama, J.; Miles, M. J. *J. Struct. Biol.* **1997**, *119*, 129–138.
(11) Baker, A. A.; Helbert, W.; Sugiyama, J.; Miles, M. J. *Appl. Phys. A* **1998**, *66*, S559–S563.
(12) Kontturi, E.; Tammelin, T.; Osterberg, M. *Chem. Soc. Rev.* **2006**, *35*, 1287–1304.
(13) Habibi, Y.; Foulon, L.; Aguié-Béghin, V.; Molinari, M.; Douillard, R. *J. Colloid Interface Sci.* **2007**, *316*, 388–397.
(14) Heiner, A. P.; Teleman, O. *Langmuir* **1997**, *13*, 511–518.
(15) Yamane, C.; Aoyagi, T.; Ago, M.; Sato, K.; Okaji Ma, K.; Takahashi, T. *Polym. J.* **2006**, *38*, 819–826.
(16) Clarke, A. J. In *Biodegradation of Cellulose: Enzymology and Biotechnology*; Technomic Pub. Co.: Lancaster, PA, 1997.

containing the catalytic domain and the cellulose-binding module (CBM) is extended and tail-like. The protein is approximately 20 nm in length.[17−19] Previous studies have indicated that CenA attacks susceptible linkages in soluble carboxymethyl cellulose (CMC) in a relatively random manner.[20] CenA has one CBM characteristic of family 2 of the CAZy organizational system that is approximately 100 amino acids long.[17] The ability of CenA to hydrolyze cellulose depends on the cellulose source. For cotton, CenA decreases the degree of polymerization of the residual insoluble substrate progressively; however, it leaves a low-molar-mass product in the later stages of digestion.[21] On bacterial cellulose, CenA has a similar action but it releases two products of different mean molar mass. On bacterial microcrystalline cellulose, CenA is significantly less active and also releases two products of different mean molecular mass. The degree of crystallinity of these three substrates varies in the sequence cotton < bacterial cellulose < bacterial microcrystalline cellulose. The activity of CenA on each substrate varies in the sequence cotton ≥ bacterial cellulose ≥ bacterial microcrystalline cellulose.[21,22] These results suggest that CenA preferentially attacks amorphous regions in the cellulose microfibrils.[22]

Cellulose−enzyme interactions have most often been investigated by biochemical and microbiological techniques[16,20] and electron[1−3] and fluorescence microscopy.[23,24] To date, AFM has not been used to study in situ binding and degradation events of enzymes on a native cellulose substrate. In this article, we present the first results of the use of AFM to investigate these events on a native substrate, which allows us to measure directly the interactions of enzymes with cellulose fibers in a liquid environment. The use of intermittent contact AFM minimized the sample−tip interactions while maintaining optimal conditions for the enzymatic reactions. High-resolution AFM imaging allows for the direct observation and measurement of enzyme activity, which provides insight into the mechanism of cellulose digestion by enzymes at the single-molecule level. There are additional elements of novelty in this study. We developed a protocol that allowed us to image single cellulose fibers in a film that was never dried. We have also applied the tip deconvolution procedure to remove the tip-broadening effect from the AFM images.

Materials and Methods

Reagents and Solutions. The self-assembly of monolayers of 1-thio-D-glucose has been previously described by Revell[25] and Mandler.[26] An approximately 2 mmol L^{-1} solution was prepared with 2 mg of 1-thio-D-glucose (Sigma) or thioglycerol (99.0%, BioChemika, Fluka) and spectroscopic-grade methanol (99.96%, Fisher Scientic). Fresh solutions of the thiols were prepared for all experiments to minimize contamination. The electrolyte for enzyme experiments was potassium phosphate buffer (pH 7.4). The buffer was prepared using 0.17 g monobasic, anhydrous KH_2PO_4 (99.99%, Sigma-Aldrich), and 0.51 g dibasic anhydrous K_2HPO_4 (99.99%, Sigma) in 100 mL of Milli-Q ultrapure water (resistivity 18.2 MΩ).

Cellulose Preparation. Cellulose was grown from the bacterium *A. xylinum* for approximately 1 month in a quiescent solution.[27] To prepare the cellulose dispersion, glass beads, 2.5 mm in diameter, were used in a ball milling process (BeadBeater by Biospec Products Inc.). Approximately 200 mg of cellulose was added to the small chamber that was filled to two-thirds capacity with glass beads. Methanol was added carefully to the chamber to avoid air-bubble formation. The BeadBeater was run for 2 min and then allowed to cool for 10 min. This procedure was typically repeated three times or until an even slurry was obtained.

The beads and cellulose were emptied from the chamber into a small crystallizing dish, and the chamber was washed three times with methanol. The cellulose created a suspension in the methanol and could be decanted with a Pasteur pipet as the beads sank to the bottom of the dish. The beads were washed five times with 10−20 mL aliquots of methanol, and all of the remaining cellulose was collected. Three 1.5 mL samples of the cellulose dispersions were dried in glass weighing boats. The concentration of the methanol dispersion was determined to be approximately 10 mg mL^{-1}.

Enzyme Solution. Details for the preparation and purification of recombinant CenA endoglucanase from *Cellulomonas fimi*[28] will be described elsewhere. Briefly, the *cenA* gene (kindly provided by RAJ Warren) was subcloned into pET30a(+) to provide the protein product with a C-terminal hexa-His tag. *Escherichia coli* BL21(DE3) competent cells were freshly transformed with the plasmid and incubated in Luria−Bertani broth containing 50 μg/mL Kan at 37 °C with aeration. In the mid-exponential phase of growth (o.d. 600 nm of approximately 0.6), the expression of *cenA* was induced with the addition of 1 mM IPTG (final concentration). Following further incubation of cells at 37 °C for 3 h, the cells were harvested by centrifugation (5000*g*, 12 min, 4 °C), resuspended in IMAC buffer (50 mM sodium phosphate buffer, pH 8.0, 300 mM NaCl) containing complete EDTA-free protease inhibitor cocktail tablets, 10 μg/mL RNase I, and 5 μg/mL DNase I, and incubated on ice for 30 min prior to disruption with a sonicator ultrasonic liquid processor (Heat Systems Inc., Toronto, ON, Canada) fitted with a macroprobe. The resulting cell lysate was clarified by centrifugation (5000*g*, 15 min, 4 °C), and overproduced CenA was purified to apparent homogeneity (as determined by SDS PAGE) using a combination of immobilized metal affinity and anion-exchange chromatography as previously described.[29] The recovered CenA was dialyzed overnight at 4 °C against 2 × 1 L of 50 mM sodium phosphate buffer at pH 7.4 and made up to approximately 0.1 mg mL^{-1}, but concentrations were either increased or decreased depending on the requirements of a specific experiment. The enzyme samples were freshly prepared for each experiment but were found to be stable for 5 days.

Endoglucanase activity was routinely measured by monitoring the release of reducing sugars over time from a 0.4% solution of carboxymethyl cellulose in 50 mM sodium phosphate buffer at pH 7.4 using the Nelson Soymogi assay.[30]

Langmuir−Blodgett Measurements. All cellulose films were prepared using the Langmuir−Blodgett technique using a KSV 5000 Langmuir−Blodgett trough. The Wilhelmy plate method was used to measure the surface pressure $\Pi = (\gamma_o - \gamma_c)$ at the gas/solution interface, where γ_c is the surface tension at the gas/solution interface in the presence of a film and γ_o is the surface tension in the absence of a film. The Wilhelmy plate was a piece of clean filter paper (recommended by the KSV 5000 user manual) connected to a

(17) Shen, H.; Schmuck, M.; Pilz, I.; Gilkes, N.; Kilburn, D.; Miller, R., Jr; Warren, R. *J. Biol. Chem.* **1991**, *266*, 11335–11340.
(18) Din, N.; Forsyth, I. J.; Burtnick, L. D.; Gilkes, N. R.; Miller, R. C.; Warren, R. A. J.; Kilburn, D. G. *Mol. Microbiol.* **1994**, *11*, 747–755.
(19) Pilz, I.; Schwarz, E.; Kilburn, D. G.; Miller, R. C.; Warren, R. A.; Gilkes, N. R. *Biochem. J.* **1990**, *271*, 277–280.
(20) Stalbrand, H.; Mansfield, S. D.; Saddler, J. N.; Kilburn, D. G.; Warren, R. A. J.; Gilkes, N. R. *Appl. Environ. Microbiol.* **1998**, *64*, 2374–2379.
(21) Jeffries, T. W., Viikari, L., Eds. In *Enzymes for Pulp and Paper Processing*; ACS Symposium Series; American Chemical Society: Washington, DC, 1996; p 64.
(22) Kleman-Leyer, K. M.; Gilkes, N. R.; Miller, R. C., Jr; Kirk, T. K. *Biochem. J.* **1994**, *302*, 463–469.
(23) Linder, M.; Winiecka-Krusnell, J.; Linder, E. *Appl. Environ. Microbiol.* **2002**, *68*, 2503–2508.
(24) Blake, A. W.; McCartney, L.; Flint, J. E.; Bolam, D. N.; Boraston, A. B.; Gilbert, H. J.; Knox, J. P. *J. Biol. Chem.* **2006**, *281*, 29321–29329.
(25) Revell, D. J.; Knight, J. R.; Blyth, D. J.; Haines, A. H.; Russell, D. A. *Langmuir* **1998**, *14*, 4517–4524.
(26) Burshtain, D.; Mandler, D. *Phys. Chem. Chem. Phys.* **2006**, *8*, 158–164.
(27) Delmer, D. P. *Annu. Rev. Plant Physiol.* **1999**, *50*, 245–276.
(28) Gilkes, N.; Warren, R.; Miller, R., Jr; Kilburn, D. *J. Biol. Chem.* **1988**, *263*, 10401–10407.
(29) Scheurwater, E. M.; Clarke, A. J. *J. Biol. Chem.* **2008**, *283*, 8363–8373.
(30) Nelson, N. *J. Biol. Chem.* **1944**, *153*, 375–380.

microbalance (KSV-Instruments). Plots of the surface pressure versus the trough area were used to determine the optimum surface pressure for film transfer.

Cellulose thin films were transferred at different surface pressures using the dipping configuration of the Langmuir−Blodgett trough.

AFM Measurements. AFM images were collected using a Pico SPM Microscope with an AFMS 182 scanner and the Picoscan 5.2 software system using silicon nitride tips that had a nominal spring constant of 0.20 N m^{-1} (Digital Instruments) in contact mode and 2.8 N m^{-1} for magnetically coated silicon tips in MAC mode (type II, Molecular Imaging). The contact-mode tips were exposed to ozone in a UV laminar flow cabinet for 30 min prior to use. All images were acquired in deflection mode with both integral and proportional gains close to 1 using scan rates of 1 to 3 lines/s. In AFM experiments, the substrate consisted of a 200-nm-thick gold film vapor deposited onto a glass slide pretreated by the deposition of a 2-nm-thick layer of chromium to ensure better adhesion of the gold to the glass substrate. The electrode was annealed in a muffle furnace at 700 °C for a period of 60 s prior to each experiment.

The homemade AFM liquid cell was equipped with capillary ports for the addition of enzyme for in situ imaging experiments. All in situ imaging was carried out at room temperature, 20 ± 2 °C, using MAC-mode AFM to minimize lateral forces. Strong lateral forces, such as those used in contact mode, are known to dislodge loosely adsorbed objects from the substrate.

For all in situ AFM enzyme experiments, a stable image of cellulose fibrils was obtained before introducing the enzyme. The tip was then moved away from the surface using the amplitude setpoint control, and the enzyme solution flowed into the cell. The tip was reengaged with the sample and imaged immediately after the addition of enzyme. Following the collection of an AFM image, the sample was left undisturbed for 2−5 min before the next image was recorded.

For all MAC-mode AFM measurements, topography, amplitude, and phase-mode images were obtained simultaneously. By combining the three imaging modes, a more complete understanding of the sample can be obtained. Amplitude images often highlight features that are not easily seen in topography images, and phase images provide information about the energy dissipation[31] between the tip and the sample, resulting in a map of the relative stiffness of the sample. All quantitative measurements were performed on the topography images only. Fibril diameter measurements were obtained by taking the average fibril width from numerous cross-sectional measurements along a single fiber.

The most prevalent complication in AFM imaging is image drift, which makes the tracking of single cellulose fibers difficult and impedes the collection of quantitative data. One of the major contributing factors is thermal drift in the piezoelectric scanner as a result of external temperature changes. We attempted to minimize drift by allowing the AFM setup with the liquid cell attached to equilibrate for 1 to 3 h before the enzyme experiments were performed. This significantly decreased the drift but did not eliminate it entirely.

The presence of gold terraces on the underlying substrate allowed the identification of reference features that were independent of enzymatic degradation of cellulose fibers and served as a convenient way to compensate for drift and to track a single cellulose fiber. The scanning speed has a measurable effect on the quality of the image; it is important to scan fast enough that events are not missed but slow enough that tip interactions do not have a detrimental effect on the measured topography of the sample. The scan speed used in all experiments was 2 to 3 Hz.

Results and Discussion

Cellulose Fibril Characterization. The Langmuir−Blodgett technique was chosen to prepare thin films of cellulose fibers because it forms films reproducibly. Because cellulose does not dissolve in any typical solvent, the cellulose fibers were dispersed in methanol/chloroform (1:5). The dispersion concentration was ~2 mg mL^{-1}. In typical Langmuir−Blodgett (LB) experiments, the change in surface pressure is plotted against the change in the area per molecule. The pressure−area isotherm is then the 2D equivalent of the pressure−volume isotherm. In the case of cellulose dispersions, the area per fiber is variable and unknown. Therefore, the change in surface pressure was plotted against the change in the area of the trough as the film was compressed. This type of plot was used previously by Yang et al.[32] in experiments with silver nanowires dispersed at the air/water interface. Such pressure−area isotherms are working curves that are used to determine the optimal conditions for reproducible film transfer, and they are not used to determine any physical parameters.

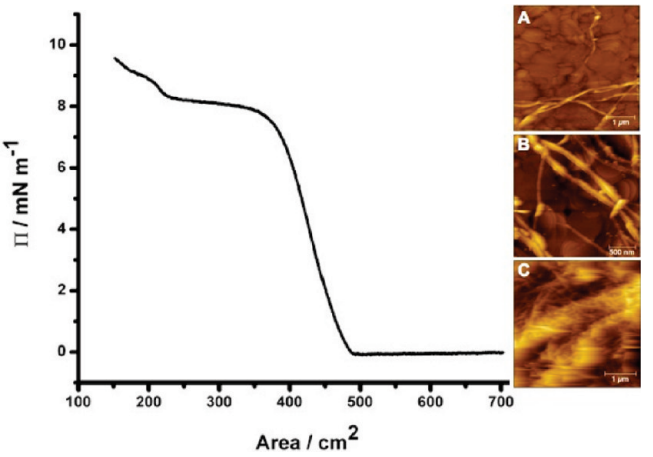

Figure 1. Surface pressure−LB trough area isotherm of bacterial cellulose ball milled in methanol and suspended in chloroform. Insets are topography MAC-mode AFM images of cellulose fibers transferred at (A) 2, (B) 5, and (C) 8 mN m^{-1}.

A typical surface pressure−LB trough area isotherm, prepared by spreading 1 mL of a 2 mg mL^{-1} bacterial cellulose dispersion at the air/water interface and allowing the solvent (methanol/chloroform) to evaporate for 30 min, is shown in Figure 1. The zero value of the surface pressure during the initial stages of compression indicates that the cellulose fibers are well dispersed at the water−air interface and the film is very compressible. At higher compression, the surface pressure increases. To determine the best conditions for the transfer of fibers, the LB deposition of cellulose onto the gold-coated glass slides was performed at a few selected film pressures. To improve the adhesion of cellulose fibers, the gold surface was chemically modified by a self-assembled monolayer of a hydrophilic thiol. The samples were then mounted into the AFM liquid cell for imaging. The cell was filled with water, and images were acquired for the sample in the aqueous environment. In general, higher resolution is achieved when fibrils are imaged in solution than in air as a result of the elimination of capillary forces.[33]

In Figure 1, images A−C are the topography MAC-mode AFM images of the structure of the film transferred onto the gold-coated glass slide at different surface pressures. The image in Figure 1A shows that at a film pressure of 2 mN m^{-1} the aerial density of the fibers is so low that it is difficult to find the fiber on the substrate surface. At a film pressure of 8 mN m^{-1} (image in Figure 1C), the aerial density of the fibers is too large. The image

(31) Cleveland, J. P.; Anczykowski, B.; Schmid, A. E.; Elings, V. B. *Appl. Phys. Lett.* **1998**, *72*, 2613–2615.

(32) Yang, P. *Nature* **2003**, *425*, 243–245.

(33) Meyer, E.; Hug, H. J.; Bennewitz, R. In Scanning Probe Microscopy: The Lab on a Tip; Advanced Texts in Physics, 1439−2674; Springer: Berlin, 2004.

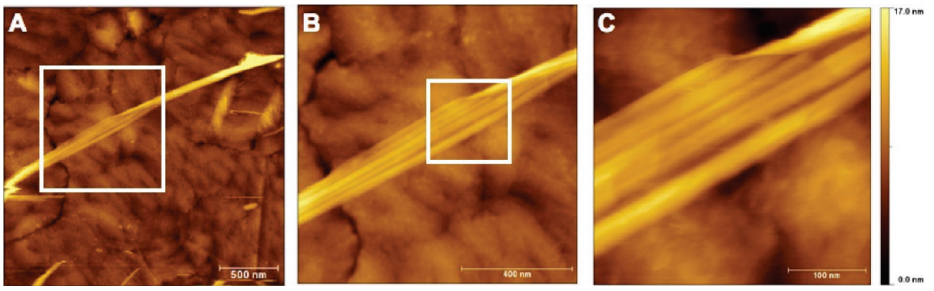

Figure 2. MAC-mode AFM topography images of typical cellulose fibers anchored with 1-thio-D-glucose on gold imaged in water. (A) Typical fibers. (B) Higher-resolution image corresponding to the white box shown in part A. (C) Higher-resolution image corresponding to the white box shown in part B, which shows a fiber composed of bundles of fibrils. The tip -deconvolution procedure was applied to remove the tip-broadening effect from the images.

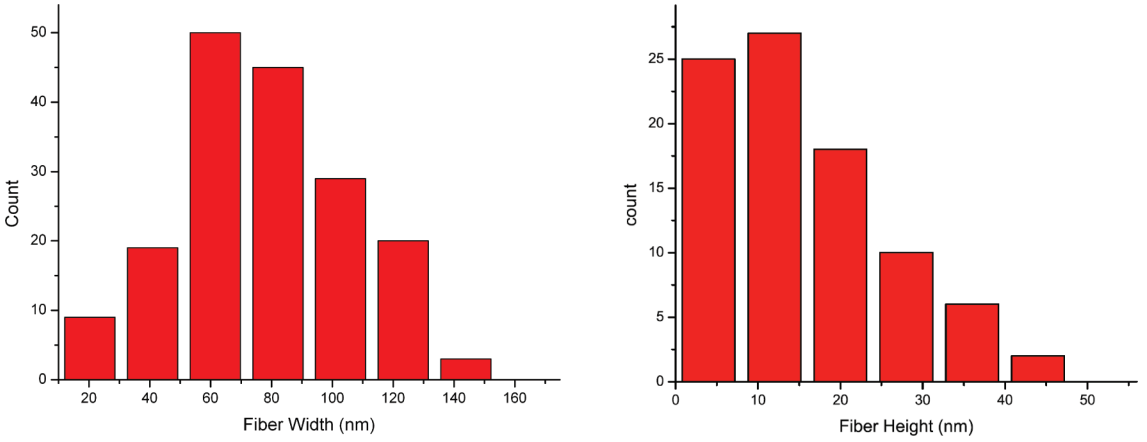

Figure 3. Histograms of fiber widths and heights (nm) measured on 85 fibers in 21 different AFM images for never-dried samples after the tip-deconvolution procedure.

in Figure 1B shows that the compression of the cellulose dispersion at 5 mN m^{-1} is ideal for yielding a large number of isolated fibers.

Biological molecules imaged using AFM must be adsorbed firmly to a substrate. The initial preparation protocol included drying the sample under vacuum for 24 h prior to imaging. By allowing the cellulose sample to dry prior to measurements in fluid, the stability of the film was increased, with the sample remaining stable under water for several days. Edgar and Gray noted a similar phenomenon in their study of cellulose films: oven drying of the films increased their stability against mechanical agitation.[34] Revol et al[35] has also noted this phenomenon. Although the stability of the film is desirable for imaging purposes, drying under vacuum or heating cellulose fibers has an adverse effect on the activity of enzymes on the cellulose substrate. Cellulose fibers that have never been dried are most susceptible to enzymatic attack.[36,37] Because of this, large-scale operations of converting cellulose biomass into ethanol use fibers that have never been dried. Hence, it was advantageous to develop a sample-preparation protocol that avoids drying cellulose fibers while maintaining strong adhesion of the fibers to the substrate so that the enzymatic action on a single fiber can be imaged repeatedly using AFM.

To achieve this goal, the following protocol was used. First, 1-thio-D-glucose-modified gold substrates were used because this molecule has a stronger affinity to cellulose than thioglycerol and hence better adhesion of the cellulose fibers to this surface was expected. Second, MAC mode, an intermittent tapping mode, was chosen as the imaging technique to minimize the forces acting on the sample. Figure 2A−C shows topographical images of an individual fiber at progressively higher magnification transferred onto the substrate without drying at a compression of 5mN m^{-1}. In these images, a single cellulose fiber is imaged and gold terraces are visible under the fiber so that they could be used as fiducial marks for the determination of the fiber width and height.

When the dimensions of the imaged fibers are comparable in magnitude to the dimensions of the AFM cantilever tip, the sample image is convoluted with the tip geometry and the result is a broadening of the lateral dimensions of the topographical image of a single fiber. In Figure 2, tip deconvolution was performed to account for this effect. An example of such deconvolution was described by Markiewicz and Goh.[38] In this work, we employed the deconvolution module in commercial software SPIP (ImageMetrology Ltd., Denmark) using the blind construction algorithm. Scanning electron microscopy was used to determine the tip geometry. The tip had a conical shape, and its radius of curvature was 15 nm. In the deconvoluted images, the fibers are narrower than in the original AFM image. Figure 3 shows a histogram of the width and the height of individual fibers in the deconvoluted images. The fibers are 73 ± 37 nm wide. The average height is ~15 nm, which is significantly smaller than the width, indicating that the fibers are ribbon-shaped. A comparison of histograms for never-dried and dried samples is given in Figures SI 1 and SI 2 of the Supporting Information.

(34) Edgar, C. D.; Gray, D. G. *Cellulose* **2003**, *10*, 299–306.
(35) Revol, J.-F.; Bradford, H.; Giasson, J.; Marchessault, R. H.; Gray, D. G. *Int. J. Biol. Macromol.* **1992**, *14*, 170–172.
(36) Wood, T. M.; Saddler, J. N. *Method. Enzymol.* **1988**, *160*, 3–11.
(37) Akishima, Y.; Isogai, A.; Kuga, S.; Onabe, F.; Usada, M. *Carbohydr. Polym.* **1992**, *19*, 11–15.
(38) Markiewicz, P.; Goh, M. C. *Langmuir* **1994**, *10*, 5–7.

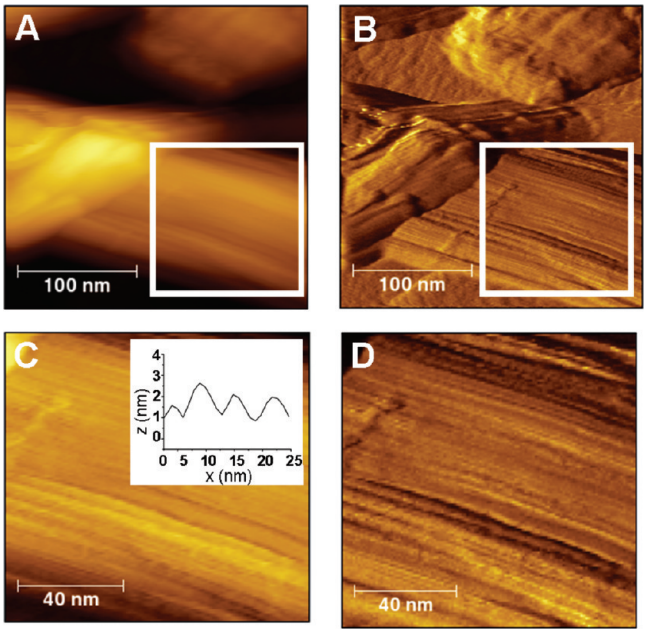

Figure 4. High-resolution MAC-mode AFM images; topographic (A, C) and amplitude (B, D) images of cellulose fibers and microfibrils.

The high-resolution MAC-mode AFM images in Figure 4 reveal the fine structure of the cellulose fibers that consist of parallel stacks of microfibrils. Figure 4A,C was acquired using the topographic mode of detection, and Figure 4B,D shows simultaneously recorded images using amplitude detection. Amplitude detection gives a better contrast, but the topographic images can be used to determine the dimensions of the microfibrils. The inset of Figure 4C plots the height−distance profile in the direction normal to the fiber. This profile shows a corrugation of the fiber surface with a periodicity 5 ± 1 nm and a peak-to-peak amplitude of ~1 nm. An AFM tip with a radius of curvature of 15 nm cannot provide a precise profile of the surface roughness. However, the periodicity of the surface features is convoluted with the tip displacement, and the lateral dimensions of surface corrugation can be determined precisely with such a tip.[39]

Most of the information concerning the structure of the cellulose fibers has been obtained from transmission electron microscopy (TEM) or X-ray scattering studies[40−45] performed on dried cellulose fibers. There is quite a spread in the reported dimensions of the fibers and microfibrils. For example, for *A. xylinum* cellulose, Iguchi et al.[44] reported a ribbon cross section of 80×4 nm^2 and microfibril dimensions of 2−4 nm. Tokoh et al.[45] estimated that the ribbons are 30 to 50 nm wide and 6 to 10 nm thick and consist of microfibrils that are 6 to 10 nm wide. In AFM studies by Yamanaka et al.,[41] the *A. xylinum* cellulose fibers were on average 117 nm wide, with the width ranging from 98 to 140 nm, and on average 4 nm thick. This data was not corrected for the tip-broadening effect. The only structural studies on wet samples were performed by Astley et al.[46] Using environmental scanning electron microscopy, they estimated the width of the *A. xylinum* cellulose fibers to be ~50 nm. However, the resolution of their images was 1 or 2 pixels per 50 nm and hence was comparable to the reported value of the fiber width. From small-angle X-ray scattering experiments, they determined that the average cross-section of the microfibril is equal to 1×16 nm^2. However, this number was derived from the poor fit of a model to the experimental data with significant scatter and hence cannot be trusted. The results presented in our work are much more precise. Our estimate of the cross section of the microfibril in the wet sample is $5 \pm 1 \times 5 \pm 1$ nm^2. Furthermore, we demonstrated that there is a significant spread in the values of fiber width and thickness and that it is not appropriate to represent them with a single value. For example, the fiber in Figure 2 is about 100 nm wide and ~4 nm thick but it consists of ~20-nm-wide ribbons stitched together. It is also twisted and the fiber dimensions and thickness are changing along its length. The procedure to image never-dried cellulose sample will now be applied to investigate the enzymatic attack on individual fibers.

Real-Time Imaging of Enzymatic Cellulose Degradation Using Liquid-Phase AFM. The enzymatic digestion of the cellulose fibers was studied using bacterial cellulose films deposited on 1-thio-D-glucose-modified gold substrates in phosphate buffer at pH 7.4 (herein referred to as the buffer) at room temperature, 20 ± 2 °C. CenA endoglucanase from C. *fimi* enzyme was added to the AFM cell to investigate the degradation of the native cellulose sample. Two types of control experiments were performed to determine that the resulting degradation was actually due to the addition of enzyme and was not due to mechanical disruption or the delamination of the sample. First, a cellulose sample in the absence of added enzyme was imaged repetitively in the same spot for 3 h. Figure SI 3 in the Supporting Information shows that there is no significant change in the sample topography, indicating that the mechanical wear from the tip−sample interactions does not play a major role in the experiment. In the second control, a cellulose sample was imaged in the buffer solution and then left to stand in the buffer overnight. The sample was imaged again the next morning. There was no significant topographical change, indicating that the sample did not degrade in the buffer solution without enzyme. These controls assured us that, in the presence of the enzyme, any changes in the fiber topography will be a result of enzymatic action on the cellulose fibers.

Figure 5A−F shows the progression of enzyme action on the cellulose fiber observed over a period of almost 9 h. Figure 5A is a high-resolution image of a bundle of three fibers recorded before the addition of enzyme. To facilitate further discussion, we have numbered these fibers (see the labels in Figure 5) and labeled a reference gold terrace with a blue "X". Fiber 3 is quite smooth and defect-free. In contrast, fiber 2 has visible defects in the bottom right corner and a less visible but discernible defect on the left upper edge. Fiber 1 is very short, and the irregular shape of its end indicates the presence of many defects. The enzyme solution was then injected into the AFM cell without disengaging the set point of the AFM tip. Figure 5B shows an image of the three fibers acquired 3 min after enzyme injection. The enzyme molecules are moving quickly, traveling a distance approximately equal to several hundred cellobiose units per minute (diffusion coefficient ~3×10^{-11} cm^2/s).[47] Hence, their movement on the cellulose

(39) Mate, C. M.; McClelland, G. M.; Erlandsson, R.; Chiang, S. *Phys. Rev. Lett.* **1987**, *59*, 1942–1945.
(40) Steinbüchel, A.; Hofrichter, M. *Biopolymers*; Wiley-VCH: Weinheim, Germany, 2001; p 37.
(41) Yamanaka, S.; Ishihara, M.; Sugiyama, J. *Cellulose* **2000**, *7*, 213–225.
(42) Ross, P.; Mayer, R.; Benziman, M. *Microbiol. Mol. Biol. Rev.* **1991**, *55*, 35–58.
(43) Haigler, C. H. In *Cellulose Chemistry and its Applications*; Nevell, T. P., Zeronian, S. H., Eds.; Ellis Horwood: Chichester, U.K., 1985; p 67.
(44) Iguchi, M.; Yamanaka, S.; Budhiono, A. *J. Mater. Sci.* **2000**, *35*, 261–270.
(45) Tokoh, C.; Takabe, K.; Fujita, M.; Saiki, H. *Cellulose* **1998**, *5*, 249–261.
(46) Astley, O. M.; Chanliaud, E.; Donald, A. M.; Gidley, M. J. *Int. J. Biol. Macromol.* **2001**, *29*, 193–202.
(47) Jervis, E. J.; Haynes, C. A.; Kilburn, D. G. *J. Biol. Chem.* **1997**, *272*, 24016–24023.

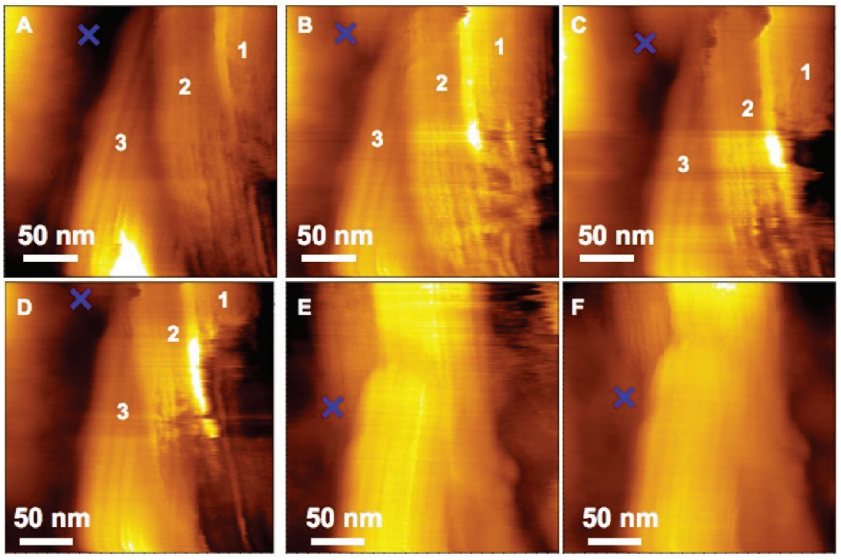

Figure 5. MAC-mode AFM topography images of a cellulose fiber after the addition of CenA endoglucanase to the AFM liquid cell. (A) Target fiber bundle before enzyme and (B) 3 min, (C) 30 min, (D) 60 min, (E) 3 h, and (F) 8.5 h after the addition of enzyme.

fibers is too fast to see individual enzymes in the AFM images. The image reveals that, whereas fiber 3 remains intact, the defects in fiber 2 are more pronounced and there is a clear degradation of fiber 1, which frays from the bottom upward as the enzyme acts on it. Figure 5C illustrates that, after 30 min, fiber 1 has been significantly shortened and the frayed edges of fiber 2 indicate that the digestion of this fiber has progressed. Figure 5D demonstrates that only small pieces of fibers 1 and 2 remained after 60 min and they are totally absent in Figure 5E, which was recorded after 3 h of enzyme exposure. Figure 5F illustrates that no change in the shape of fiber 3 (that was initially defect-free) was observed after almost 9 h of enzyme exposure. The experimental results shown in Figure 5 demonstrate clearly that CenA endoglucanase digests fibers with defects. It preferentially acts not only at the end of the fiber, where the defect density is highest, but also in areas with defects in the middle of the fiber.

The effectiveness of CenA endoglucanase on the defect sites on cellulose fibers is illustrated further by the images shown in Figure 6A−D. Figure 6A is an image of a single fiber before the addition of enzyme. It has a visible kink in the middle of the fiber that must correspond to large stress in the fiber. Evidence of this stress can be seen by the presence of faint but visible lines that lie perpendicular to the fiber direction. In the image shown in Figure 6B that was recorded 6 min after the addition of enzyme, the AFM tip adheres more strongly to the kinked area of the fiber. Figure 6C reveals that after 45 min of enzymatic action the cellulose fiber is frayed in the vicinity of the kink. After an additional 5 min, the frayed part of the fiber is fully detached because it is no longer visible in the image and the fiber in the kink area is visibly narrower than it was originally. The fiber width decreased from ~80 nm in the image in Figure 6A to ~70 nm in the image in Figure 6D, indicating a loss of cellulose mass. The changes of the fiber morphology after 45 and 50 min of the experiment can be seen more clearly in the images acquired with the phase mode shown in Figure SI 4 of the Supporting Information. The stress lines are also more visible in the phase images. It should be emphasized that the changes observed in Figure 6 are caused by the enzyme and are not AFM tip-related effects. Control experiments were performed on single fibers in the absence of the enzyme. One such experiment is shown in Figure SI 3 of the Supporting Information. These controls

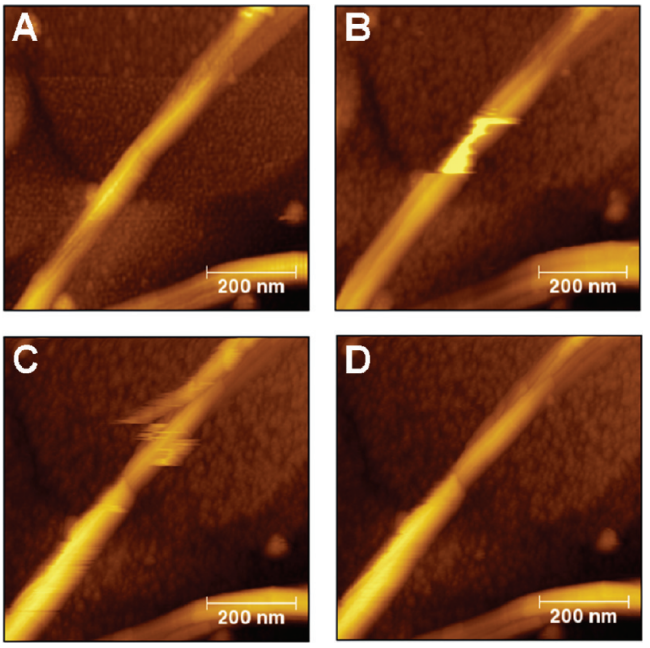

Figure 6. MAC-mode AFM topography images of a cellulose fiber after the addition of CenA endoglucanase to the AFM liquid cell: (A) before enzyme addition, (B) 6 min after enzyme addition, (C) 45 min after enzyme addition, and (D) immediately after fiber detachment.

demonstrate that in the absence of the enzyme the tip had no effect on the fiber after prolonged repetitive scanning of the tip over the fiber.

The mechanism of enzymatic attack on cellulose fibers has been investigated by several authors. Kleman-Leyer et al.[22] studied changes in the degree of polymerization during the enzymatic digestion of cellulose. These studies concluded that CenA preferentially attacks the amorphous sites and much more slowly degrades the crystalline regions. Consequently, after 24 h, they found that the hydrolysis of cellulose fibers by CenA is incomplete, with only 12% of the initial bacterial cellulose mass degraded. The preferential attack of the amorphous regions by other cellulases was also observed in transmission electron

microscopy (TEM) images of cellulose fibers transferred from a solution to a TEM vacuum chamber.[1,2,48] In addition to the hydrolysis of the amorphous regions, it has also been demonstrated that CenA has other effects on the fibers such as fiber swelling,[49] defibrillation, and the production of short fibers.[18] The results of the present study are consistent with these observations. In Figure 6, the width and thickness of the bottom section of the long fiber increase from 72 to 100 nm and from 12 to 26 nm, respectively, indicating that the fiber swells. In contrast, the width and thickness of the top segment that undergoes defibrillation decrease from 78 to 72 nm and from 20 to 17 nm, respectively.

The novelty of our work is the demonstration that AFM imaging can be used to observe such a preferential attack directly in real time and to identify the specific sites such as kinks or damaged areas of the fiber that are attacked by the enzyme. This approach offers the unique opportunity to study differences in the enzymatic digestion of cellulose from different sources and to observe selectivity in the activity of different families of enzymes. One of the greatest strengths of this technique lies in the potential to use it with technical substrates. This technique allows the identification of different cellulose isomorphs and hence the observation of enzyme interactions with those isomorphs. AFM is able to provide a spatial map of the distribution of cellulose and lignin in technical substrates and to identify cellulases that have particular affinity to these different cellulose structures or isomorphs.

(48) Boisset, C.; Chanzy, H.; Henrissat, B.; Laned, R.; Shoham, V.; Bayer, E. A. *Biochem. J.* **1999**, *340*, 829–835.

(49) Josefsson, P.; Henriksson, G.; Wagberg, L. *Biomacromolecules* **2008**, *9*, 249–254.

Conclusions

We have described the first real time in situ AFM measurements of the enzymatic attack on a single cellulose fiber. A novel protocol for preparing reproducible native cellulose films without drying the sample has been developed and successfully applied in this study. We have demonstrated the tremendous potential of AFM in studying the mechanism of the enzymatic digestion of cellulose and in identifying the most effective enzymes for the digestion of various cellulose structures or isomorphs. This approach should be particularly promising to understanding the mechanism of enzymatic hydrolysis of technical cellulose.

Acknowledgment. This work has been supported by an NSERC strategic grant (STPGP 336882) to A.J.C. We acknowledge many stimulating discussions with Drs. John Tomashek and Chris Hill of Iogen Inc. J.R.D. and J.L. acknowledge Canada Research Chair Awards.

Supporting Information Available: Histograms of the fiber width and height of dried and never-dried films. MAC-mode AFM topographic image of never-dried cellulose fibers imaged repetitively in the same spot for 1.5 h in the absence of enzyme. MAC-mode AFM phase images of a cellulose fiber after the addition of CenA endoglucanase to the AFM liquid cell. This material is available free of charge via the Internet at http://pubs.acs.org.